Estimating reliability of blood glucose concentration predictions in patients with type 1 diabetes mellitus

Alain Bock[a], Grégory François[b], Denis Gillet[a,*]

[a] *React Group, École Polytechnique Fédérale de Lausanne (EPFL), Switzerland*
[b] *Laboratoire d'Automatique, École Polytechnique Fédérale de Lausanne (EPFL), Switzerland*

Abstract

Blood glucose concentrations of patients with type 1 diabetes mellitus are subject to very high inter- and intra-patient variability. This variability may be detrimental to the reliability of the treatment, thus resulting in potentially frequent hypo- or hyperglycemia. Model-based therapies have the potential to improve the quality of the treatment, but most of the well-accepted deterministic models of reasonable complexity are not capable of capturing intra-patient variability. The contribution of this article is to propose a method to predict individual blood glucose concentrations and the corresponding confidence intervals while accounting for inter- and intra-patient variability. For this purpose, it is proposed to construct a stochastic model by incorporating parametric uncertainty on a given continuous deterministic model and by propagating the uncertainty using the theory of the extended Kalman filter. Resulting stochastic model predictions are shown to be reliable using the FDA-approved UVa/Padova simulator and real clinical patient data. They can be used, among others, to increase safety for blood glucose control (open- as well as closed-loop), or to filter measurements.

Keywords: Type 1 Diabetes Mellitus, Blood Glucose Prediction, Stochastic Modeling, Confidence Intervals, Uncertainty

1. Introduction

Type 1 Diabetes Mellitus (T1DM) is a disease characterized by the absence of endogenous production of insulin, a hormone that stimulates the uptake of glucose from the blood into cells. This disease, originated by an autoimmune destruction of insulin-producing β-cells in the pancreas, leads to elevated Blood Glucose (BG) concentrations. This state is known as hyperglycemia and, if not or improperly treated, can cause a number of severe conditions such as blindness or nerve and cardiovascular damage [1]. The treatment of T1DM consists in infusing exogenous insulin using an insulin pump or a pen. The main challenge in this treatment lies determining the appropriate insulin dose. Overdosing insulin leads to low BG concentrations, also known as hypoglycemia, causing severe acute consequences such as losing consciousness, coma or even death. Therefore the insulin treatment needs to avoid hypoglycemia completely, while reducing hyperglycemia as much as possible - the right compromise needs to be found.

However, this treatment is greatly complicated by a large number of uncertainties:

- Inter-patient variability: Patients differ significantly from one to another and need to have an individualized treatment. These differences have physiological and life-style related reasons and are significant: inter-patient variability for insulin absorption may have a coefficient of variation (CV) between 20-45% in a clinical environment [2]. This number might even be higher for complete BG dynamics and in an out-patient setting. For this reason, model-based treatment typically requires that the model at hand is reliably identifiable *for each patient*. An example of inter-patient variability is given in figure 1.
- *Intra-patient variability*: If a single patient is set to repeat the same day several times, BG concentrations during these days may change significantly. This glucose variability is related among others to changes in insulin sensitivity, but also to insulin therapy [3]. The CV of this variability has been recently quantified and lies between 15 and 25% for insulin absorption in a clinical setting [2]. This is considerable and may lead to hypoglycemia.
- *Measurement noise*: BG measurements, when using Self Monitoring of Blood Glucose (SMBG) or Continuous Glucose Meters (CGM), are very noisy. The ISO 15197 norm prescribes that 95% of measurements should be within 20% of the exact value if the reference BG > 75 mg/dl and within ± 15 mg/dl if BG ≤ 75 mg/dl. However, neither many SMBG devices [4], nor CGMs [5] currently fulfill this norm.

*Corresponding author
Email addresses: alain.bock@epfl.ch (Alain Bock), gregory.francois@epfl.ch (Grégory François), denis.gillet@epfl.ch (Denis Gillet)

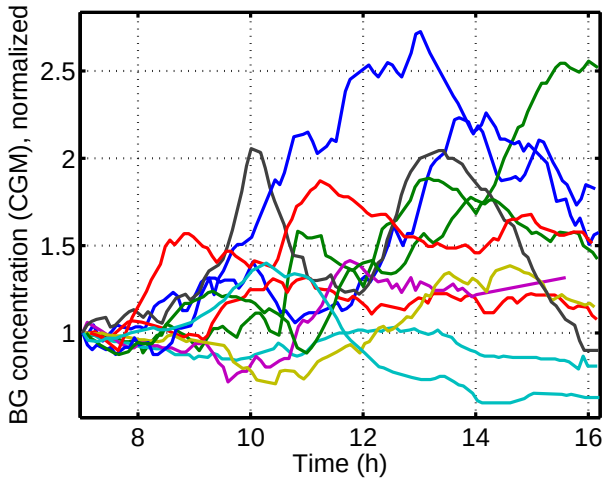

Figure 1: Example of inter-patient variability. The figure shows CGM measurements from 12 patients of a clinical study described in 4.1.2. All patients took the exact same meal under standard therapy. BG concentrations are normalized with their respective initial BG concentrations.

- *Meal announcement errors*: For most T1DM treatment methods, patients have to annouce their meals. Hence, they need to estimate the carbohydrates (CHO) content of the meal they are about to ingest. However, this estimation is prone to be difficult and even experienced patients may make considerable estimation errors. An average intra-individual variation in meal announcements of 30%, which has a significant impact on treatment outcomes, has been reported [6].
- *Meal uptake rate variability*: Depending on the type of a meal, the blood glucose apperance rate may vary considerably [7]. This variation can be quantified by means of the Glycemic Index (GI) that can be taken into account when predicting the effect of the meal. Nevertheless, this source of uncertainty remains and can mainly be addressed by using different model parameters for each kind of meal.

The combination of these uncertainties makes accurate BG predictions impossible and calls for using probabilistic approaches.

As discussed above, inter-patient variability can be accounted for by identifying individual model parameters for each patient. However, this requires models with very specific properties such as the Therapy Parameter-based Model (TPM) [8]. Meal uptake rate variability can be addressed by identifying dedicated meal parameters and constructing, e.g., a meal library [9, 7]. However, methods to quantify intra-patient variability are more difficult and rarely found in the literature. These methods aim at finding confidence intervals on predicted BG concentrations. One possibility is to apply modal interval analysis [10, 11]. With this approach, upper and lower limits on BG are computed on the basis of the deterministic model at hand and on the predetermined model parameter bounds. This method is computationally efficient, but difficult to set up. Additionally, neither experimental verification nor method to determine parameter intervals is available. Similarly, the problem was addressed by computing upper and lower bounds based on TPM parameter identification [12]. Another approach is to add process noise to transform Ordinary Differential Equations (ODEs) into Stochastic Differential Equations (SDEs) and to identify the process noise amplitude [13]. However, finding this amplitude is not straightforward. A similar approach uses a multi-model method, but is computationally demanding [14]. Finally, it is also possible to estimate uncertainties using linear regression prediction methods. However, this method is only reliable for short prediction horizons of up to 20 minutes [15].

In this article, we propose a generic and complete procedure to estimate the time-varying quality of model predictions by constructing a stochastic model and quantifying model uncertainties. The ODEs of potentially any continuous and deterministic model are transformed into SDEs by the addition of parametric uncertainties. Model parameter uncertainties are estimated during the classical parameter identification stage and, thus, no additional parameters need to be identified. These uncertainties are then propagated using Extended Kalman Filter (EKF) theory. We show that, applied to a well-chosen BG prediction model such as the TPM, this approach leads to the obtaining of confidence intervals on BG predictions.

The article is structured as follows: first, in section 2, the stochastic model, the uncertainty estimation, and the covariance propagation are introduced. Then the TPM is presented in section 3 and the proposed method is applied to it. In section 4, predictions using the stochastic TPM are done and validated using simulated and clinical data. Finally, conclusions are drawn and future work is discussed in section 6.

2. Stochastic modeling

2.1. Construction of a stochastic model

The construction of a stochastic model is based on a well-chosen deterministic model. The latter one should be continuous and expressed as:

$$\dot{\mathbf{x}}(t) = \mathbf{f}_{det}\left(\mathbf{x}(t), \mathbf{u}(t), \boldsymbol{\theta}\right), \tag{1}$$

where $\mathbf{x}$ is the vector of n states, t is the time, $\mathbf{u}$ is the m-dimension input vector, $\boldsymbol{\theta}$ is a vector containing p model parameters, and $\mathbf{f}_{det}$ is the n-dimensional vector of differentiable functions that define the model dynamics. Vectors and matrices are represented in bold. One of the states in $\mathbf{x}$ should be the BG concentration. As already mentioned in the introduction, a good BG model should lead to appropriate BG predictions. Nevertheless, because of the random nature of human glycemia, BG predictions

are rarely accurate and therefore a stochastic model can show to be useful to evaluate the quality of the deterministic predictions. For this reason, it is useful to turn the deterministic model at hand $\mathbf{f}_{det}$ into a stochastic one of the form:

$$\dot{\mathbf{x}}(t) = \mathbf{f}_{sto}\left(\mathbf{x}(t), \mathbf{u}(t), \mathbf{w}(t), \boldsymbol{\theta}\right), \tag{2}$$

where $\mathbf{w}(t) \sim \mathcal{N}(\mathbf{0}, \mathbf{Q})$, $\mathbf{Q}$ is the covariance matrix of a multivariate zero-mean Gaussian, and $\mathbf{f}_{sto}$ is the n-dimensional vector of differentiable functions that define the model dynamics. Now $\mathbf{x}(t)$ is a random variable whose distribution is propagated through time.

The biggest challenge in estimating the quality of BG predictions is to model how the uncertainty $\mathbf{w}(t)$ affects the BG concentration. Often, a zero-mean univariate Gaussian is added to the BG state and all other states remain unchanged [13]. In practice, it is difficult to choose a numerical value for this Gaussian's standard deviation σ and it requires additional and computationally important identification steps. Also, with this approach, the uncertainty is independent of model inputs, even though meal inputs are a more important source of uncertainty than insulin injections, for example.

In order to define a meaningful and easy-to-identify alternative, it is proposed to consider the parametric uncertainty of the model parameters. So, to obtain a stochastic model, $\boldsymbol{\theta}$ is replaced by a normally distributed parameter vector $\boldsymbol{\Theta}$ in equation 1, defined as

$$\boldsymbol{\Theta} \sim \mathcal{N}(\boldsymbol{\theta}, \mathbf{Q}) \tag{3}$$

$$\sim \boldsymbol{\theta} + \mathbf{w}(t) \tag{4}$$

In other words, a Gaussian term is added to every parameter Θ_i, such that $\Theta_i = \theta_i + w_i$, where $\mathbf{w} = [w_1, \ldots, w_p]^T$ has the covariance matrix $\mathbf{Q}$. Thus the uncertainty on several parameters can be correlated. The strong assumption that the parameters are normally distributed presents the biggest drawback of the proposed method, as physiological parameters are often found to be log-normally distributed [16]. However, as shown in section 4, results are convincing.

If the deterministic model is linear with respect to its parameters, equation 2 can be written as

$$d\mathbf{x}(t) = \mathbf{f}_{det}\left(\mathbf{x}(t), \mathbf{u}(t), \boldsymbol{\theta}\right) dt + \mathbf{g}\left(\mathbf{x}(t), \mathbf{u}(t), \boldsymbol{\theta}\right) d\mathbf{w}(t) \tag{5}$$

where $\mathbf{w}$ is a standard Brownian motion vector of dimension p and covariance matrix $\mathbf{Q}$, and g is a deterministic function. $\mathbf{f}_{det}$ is called the *drift* function and quantifies the deterministic part of the model, same as in equation 1. $\mathbf{g}$ is called *diffusive* function and quantifies the uncertainty of the different states.

To simulate the stochastic model, for instance, the Euler-Maruyama scheme can be used. The simulations could then be used for different Monte Carlo methods. These have the advantage of giving accurate results, but at a high computational price.

2.2. Propagating uncertainties

If the complete distribution of the states is not necessarily needed, but the propagation of its variance is sufficient, the computational burden of Monte Carlo simulations can be considerably alleviated by propagating the covariance using EKF theory [17]. The model designed in the previous section is not forcibly linear. In the case of non-linearities, finding the evolution of the states and its uncertainties needs the application of a non-linear version of a Kalman filter. For this reason, the model is linearized along the estimated trajectory and $\mathbf{A}$ and $\mathbf{L}$ are defined:

$$\mathbf{A}(t) = \left.\frac{\partial \mathbf{f}_{sto}(t)}{\partial \mathbf{x}(t)}\right|_{\hat{\mathbf{x}}(t), \mathbf{w}_0} \tag{6}$$

and

$$\mathbf{L}(t) = \left.\frac{\partial \mathbf{f}_{sto}(t)}{\partial \mathbf{w}(t)}\right|_{\hat{\mathbf{x}}(t), \mathbf{w}_0}, \tag{7}$$

where $\hat{\mathbf{x}}(t)$ is the estimated state vector $\mathbf{x}(t)$ at time t. The estimated trajectory has no process noise, hence $\mathbf{w}_0 = \mathbf{0}$. Furthermore,

$$\tilde{\mathbf{Q}}(t) = \mathbf{L}(t)\mathbf{Q}\mathbf{L}(t)^T. \tag{8}$$

The state estimation is the same as for the deterministic model and the state covariance $\mathbf{P}(t)$ propagates over time, giving the following set of equations to integrate:

$$\dot{\hat{\mathbf{x}}}(t) = \mathbf{f}_{sto}\left(\hat{\mathbf{x}}(t), \mathbf{u}(t), \mathbf{w}_0, \boldsymbol{\theta}\right) \tag{9}$$

$$\dot{\mathbf{P}}(t) = \mathbf{A}(t)\mathbf{P}(t) + \mathbf{P}(t)\mathbf{A}(t)^T + \tilde{\mathbf{Q}}(t), \tag{10}$$

where $\mathbf{w}_0 = 0$. The initial conditions for $\hat{\mathbf{x}}(t)$ are set using BG measurements and state propagation using past inputs, while the initial conditions for $\mathbf{P}(t)$ are determined by covariance propagation using past inputs.

Using the covariance matrix, the standard deviation on the BG state can be isolated and thus, its uncertainty estimated at every point in time. Furthermore, the distribution of the uncertainty of the states over time is assumed to follow a normal distribution. This is a strong assumption, but allows computing confidence intervals on BG concentration. It might not hold for models with strong non-linearities, nevertheless, if the model is linear and linearly parameterized, this is not an approximation and exact results are found.

The 95% confidence interval is defined by

$$P(\hat{x}_{BG}(t) - 1.96\sigma_{BG}(t) \leq x_{BG}(t) \leq \hat{x}_{BG}(t) + 1.96\sigma_{BG}(t)) = 0.95, \tag{11}$$

where $\hat{x}_{BG}$ is the estimated BG state and σ_{BG} is the standard deviation of $\hat{x}_{BG}$. $\sigma_{BG} = \sqrt{P_{BG}}$, where P_{BG} is the variance of $\hat{x}_{BG}$, whose value is found on the BG element of the diagonal of $\mathbf{P}$. The upper 95% confidence limit is thus $\hat{x}_{BG}(t) + 1.96\sigma_{BG}(t)$ and the lower one is $\hat{x}_{BG}(t) - 1.96\sigma_{BG}(t)$.

In order to compute the confidence intervals, $\frac{n(n+1)}{2}$ additional differential equations need to be integrated. With the n equations from the deterministic model, this leads to a total of $\frac{n(n+3)}{2}$ ODEs to be integrated over the desired time horizon.

2.3. Parameter identification

The performance of the proposed stochastic model depends largely on the quality of the vector of model parameter estimates $\boldsymbol{\theta}$ and of the covariance matrix $\mathbf{Q}$. The following paragraphs show how they can be determined.

2.3.1. Estimation of $\boldsymbol{\theta}$

A non-linear weighted least squares method that minimizes the objective function J is used to estimate $\boldsymbol{\theta}$ for a given patient:

$$J(\boldsymbol{\theta}) = \sum_{i=1}^{N} W_i (G_i - \hat{x}_{BG}(\boldsymbol{\theta}, t_i))^2 \tag{12}$$

where N is number of available BG measurements, G_i is the i-th BG measurement, W_i is the weight associated to the measurement G_i, and $\hat{x}_{BG}(\boldsymbol{\theta}, t_i)$ is the predicted BG value at the measurement time t_i.

Finally, the identification problem can be written as the following optimization problem:

$$\min_{\boldsymbol{\theta}} J(\boldsymbol{\theta}) \tag{13}$$

$$\text{s.t.} \qquad \dot{\hat{\mathbf{x}}}(t) = \mathbf{f}_{det}\left(\hat{\mathbf{x}}(t), \mathbf{u}(t), \boldsymbol{\theta}\right). \tag{14}$$

Thus, the deterministic model equations need to be integrated over an appropriate time horizon and the resulting estimated glucose state is used to compute the value of the objective function.

2.3.2. Estimation of $\mathbf{Q}$

It is proposed to use the inverse of the Fisher information matrix $\boldsymbol{\mathcal{I}}$ to estimate $\mathbf{Q}$.

The Cramér-Rao bound gives a lower bound on $\mathbf{Q}$:

$$\mathbf{Q} \geq \boldsymbol{\mathcal{I}}^{-1}. \tag{15}$$

To estimate $\mathbf{Q}$, it is assumed that the Cramér-Rao bound is attained

$$\mathbf{Q} = \boldsymbol{\mathcal{I}}^{-1}, \tag{16}$$

where $\boldsymbol{\mathcal{I}}$ is defined as

$$\boldsymbol{\mathcal{I}} = \mathbf{S}_{BG}(\boldsymbol{\theta}, t_i) \begin{pmatrix} \frac{W_1}{\sigma_1^2} & 0 & 0 \\ 0 & \ddots & 0 \\ 0 & 0 & \frac{W_N}{\sigma_N^2} \end{pmatrix} \mathbf{S}_{BG}(\boldsymbol{\theta}, t_i)^T, \tag{17}$$

and σ_i is the standard deviation of the measurement error of the i^{th} data point and:

$$\mathbf{S}_{BG}(\boldsymbol{\theta}, t_i) = \frac{\partial \hat{x}_{BG}(\boldsymbol{\theta}, t_i)}{\partial \boldsymbol{\theta}} \tag{18}$$

is the $[p \times N]$-dimensional matrix of the partial derivatives of the estimated BG concentration with respect to the parameter vector $\boldsymbol{\theta}$. They can be determined by integrating the sensitivity equations with respect to $\boldsymbol{\theta}$ at the measurement times t_i:

$$\dot{\mathbf{S}}(\boldsymbol{\theta}, t) = \frac{\partial \mathbf{f}_{det}\left(\mathbf{x}(t), \mathbf{u}(t), \boldsymbol{\theta}\right)}{\partial \mathbf{x}} \mathbf{S}(\boldsymbol{\theta}, t) + \frac{\partial \mathbf{f}_{det}\left(\mathbf{x}(t), \mathbf{u}(t), \boldsymbol{\theta}\right)}{\partial \boldsymbol{\theta}} \tag{19}$$

where $\mathbf{S}(\boldsymbol{\theta}, t) = \frac{\partial \hat{\mathbf{x}}(\boldsymbol{\theta}, t)}{\partial \boldsymbol{\theta}}$. These $n \cdot p$ equations to integrate may be computed by hand or symbolic mathematical software and are very useful to compute the gradient via forward sensitivity analysis that can be used in the minimization of J.

3. Application to the TPM

In this section, we show how the proposed method for estimating confidence intervals can be used to quantify the quality of the BG predictions by means of an application to the TPM. This is not only an example, but the TPM is recommended as an excellent choice for stochastic predictions.

3.1. TPM

The TPM is a simple linear prediction model that is identifiable using only BG measurements and was shown to have good prediction capabilities. Additionally, its parameters are strongly correlated to standard therapy parameters. If parameterized in a linear way, its equations are:

$$\dot{G}(t) = -K_x X(t) + K_g U_G(t) \tag{20}$$

$$\dot{U}_G(t) = -a_g U_G(t) + a_g U_{G,1}(t) \tag{21}$$

$$\dot{U}_{G,1}(t) = -a_g U_{G,1}(t) + a_g U_{CHO}(t) \tag{22}$$

$$\dot{X}(t) = -a_x X(t) + a_x X_1(t) \tag{23}$$

$$\dot{X}_1(t) = -a_x X_1(t) + a_x U_I(t). \tag{24}$$

where G is the BG concentration in $mg \cdot dl^{-1}$, U_G is the gut glucose absorption in $g \cdot min^{-1}$, $U_{G,1}$ the intermediate gut glucose absorption in $g \cdot min^{-1}$, X is the insulin action in $U \cdot min^{-1}$, and X_1 is the intermediate insulin action in $U \cdot min^{-1}$.

The model parameters are the meal sensitivity K_g in $mg \cdot dl^{-1} \cdot g^{-1}$, the inverse of the meal time constant a_g in min^{-1}, the insulin sensitivity K_x in $mg \cdot dl^{-1} \cdot U^{-1}$, the inverse of the insulin action time constant a_x in min^{-1}. K_x is the equivalent of the therapy parameter commonly called *correction factor* and quantifies by how much BG concentration drops per unit of injected insulin. Analogously, K_g quantifies by how much BG concentration rises per gram of ingested CHO. The therapy parameter called *insulin-to-carb ratio* is equivalent to $\frac{K_g}{K_x}$ and predicts how many units of insulin should be injected per gram of ingested CHO.

The manipulated inputs are the subcutaneous insulin infusion, U_I in $U \cdot min^{-1}$ and the carbohydrate intake rate U_{CHO} in $g \cdot min^{-1}$.

The 4-dimensional vector of model parameters vector is $\boldsymbol{\theta} = [K_g, a_g, K_x, a_x]^T$ while the 5-dimensional vector of states is defined is $\mathbf{x} = [G, U_G, U_{G,1}, X, X_1]^T$ and the 2-dimensional input vector is $\mathbf{u} = [U_{CHO}, U_I]^T$.

3.2. Stochastic model for TPM

To turn the TPM into the stochastic TPM (sTPM), $\boldsymbol{\theta}$ is replaced by its stochastic version $\boldsymbol{\Theta}$ (cf equation 4), with $\mathbf{w} = [w_{K_g}, w_{a_g}, w_{K_x}, w_{a_x}]^T$ denoting the parameter uncertainty vector. We also denote w_i the uncertainty on the i^{th} parameter. The sTPM can thus be written as:

$$\dot{G}(t) = -(K_x + w_{K_x})X(t) + (K_g + w_{K_g})U_G(t) \quad (25)$$

$$\dot{U}_G(t) = (a_g + w_{a_g})(U_{G,1}(t) - U_G(t)) \quad (26)$$

$$\dot{U}_{G,1}(t) = (a_g + w_{a_g})(U_{CHO}(t) - U_{G,1}(t)) \quad (27)$$

$$\dot{X}(t) = (a_x + w_{a_x})(X_1(t) - X(t)) \quad (28)$$

$$\dot{X}_1(t) = (a_x + w_{a_x})(U_I(t) - X_1(t)) \quad (29)$$

Since the TPM is linearly parameterized, drift and diffusion functions can be defined according to equation (5). $\mathbf{f}_{det}$ is the deterministic part of equations (25) to (29) and is thus the same as the deterministic TPM defined in equations (20) to (24):

$$\mathbf{f}_{det}(t) = \begin{bmatrix} -K_x X(t) + K_g U_G(t) \\ -a_g U_G(t) + a_g U_{G,1}(t) \\ -a_g U_{G,1}(t) + a_g U_{CHO}(t) \\ -a_x X(t) + a_x X_1(t) \\ -a_x X_1(t) + a_x U_I(t) \end{bmatrix}. \quad (30)$$

The diffusion vector function, which models the uncertainties, is given by

$$\mathbf{g}(t) = \begin{bmatrix} -w_{K_x} X(t) + w_{K_g} U_G(t) \\ -w_{a_g} U_G(t) + w_{a_g} U_{G,1}(t) \\ -w_{a_g} U_{G,1}(t) + w_{a_g} U_{CHO}(t) \\ -w_{a_x} X(t) + w_{a_x} X_1(t) \\ -w_{a_x} X_1(t) + w_{a_x} U_I(t) \end{bmatrix}. \quad (31)$$

Since the TPM is linear, the covariance propagation proposed in Section 2.2 is not an approximation, but leads to exact results. Thus, equation (6) gives

$$\mathbf{A} = \begin{bmatrix} 0 & K_g & 0 & -K_x & 0 \\ 0 & -a_g & a_g & 0 & 0 \\ 0 & 0 & -a_g & 0 & 0 \\ 0 & 0 & 0 & -a_x & a_x \\ 0 & 0 & 0 & 0 & -a_x \end{bmatrix}, \quad (32)$$

and equation 7 reads:

$$\mathbf{L}(t) = \begin{bmatrix} U_G(t) & 0 & -X(t) & 0 \\ 0 & U_{G,1}(t) - U_G(t) & 0 & 0 \\ 0 & U_{CHO}(t) - U_{G,1}(t) & 0 & 0 \\ 0 & 0 & 0 & X_1(t) - X(t) \\ 0 & 0 & 0 & U_I(t) - X_1(t) \end{bmatrix}. \quad (33)$$

It should be noted that $\mathbf{A}$ is time invariant, while $\mathbf{L}$ depends on the states. This introduces a non-linearity in the covariance propagation equations, hence evaluating the stochastic model of a linear and linearly parameterized model does not result in a set of linear equations.

The initial values for these equations may be found by propagating past model inputs. However, the initial uncertainty on the BG state, $P_{BG,0}$, should be set according to the relative accuracy of the glucose meter. For the used SMBG device, 95% of BG measurements are within $r = 10\%$ of the accurate value [4], while $r = 20\%$ for CGM data (even though this value could be higher) [18]. Hence, because the distribution is assumed to be Gaussian,

$$P_{BG,0} = \left(\frac{rG_0}{1.96}\right)^2 \quad (34)$$

where G_0 is the measured BG value at the initial time.

The whole set of equations resulting from equation (10) are given in Appendix A.

3.3. Relevance of the stochastic model

To illustrate the benefits of the stochastic model, examples, based on model parameters identified on CGM data from patients of the clinical study described in 4.1.2, are considered. Two different scenarios are analyzed whereby the patient ingests 50g of CHO one hour after the start of the experiment and applies standard therapy, i.e. he infuses the amount of insulin calculated using the insulin-to-carb ratio. The CGM measurement relative error is set to 20% (i.e. to the ISO 15197 norm) and a target BG of 100 mg/dl is used.

- *Scenario 1*: The chosen patient's effect of insulin is faster than the effect of the meal ($a_x > a_g$). The deterministic TPM predicts safe treatment, however it does not take into account any source of variability. Different realizations of the sTPM in figure 2 show that the treatment may lead to hypoglycemia in some cases. The 95% confidence interval indicates that the risk of hypoglycemia is higher than 2.5 %.
- *Scenario 2*: If the effect of the meal is faster than the one of the insulin ($a_x < a_g$), which is the case for some of the patients, there is a significant risk of hyperglycemia, as illustrated in figure 3.

These two scenarios show that there is a risk of hypo- and hyperglycemia, respectively, if standard therapy is applied. The proposed stochastic model allows to quantify this risk and may allow reducing it.

4. Stochastic model validation

4.1. Validation data

The data used to evaluate the proposed stochastic model comes from the UVa simulator and a clinical study.

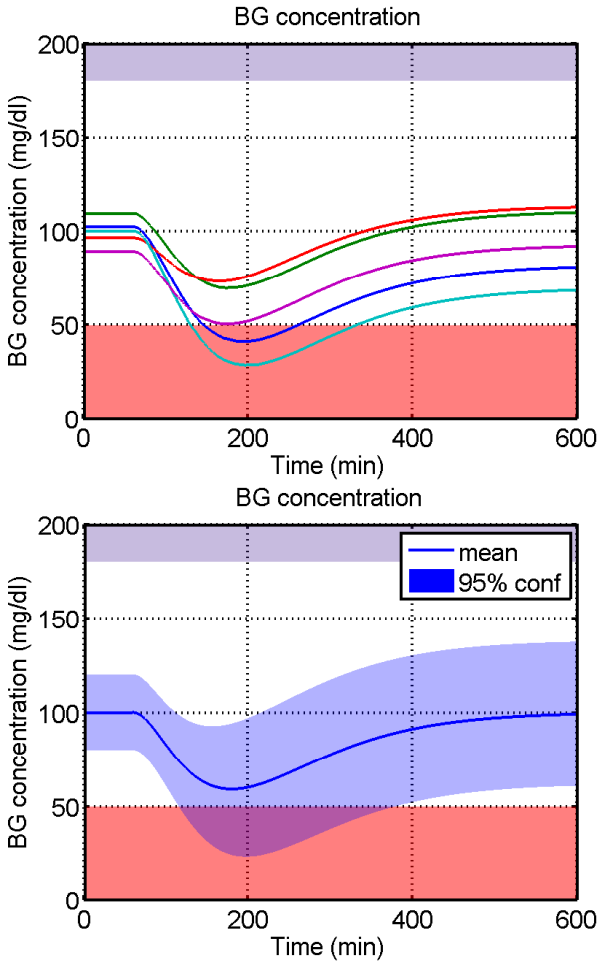

Figure 2: Scenario 1: Example of 5 realizations of the sTPM (top) and estimation of 95% confidence interval (bottom).

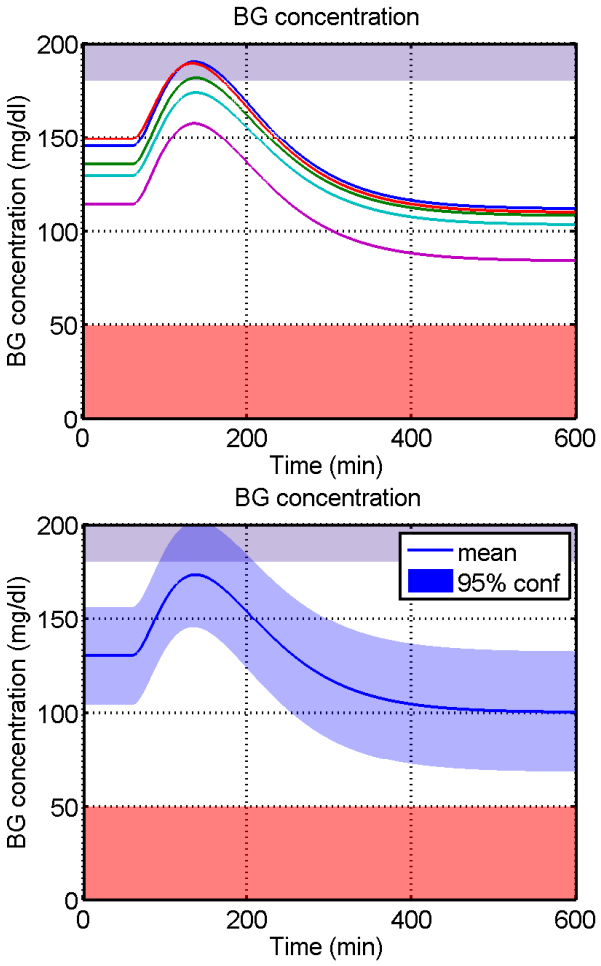

Figure 3: Scenario 2: Example of 5 realizations of the sTPM (top) and estimation of 95% confidence interval (bottom).

4.1.1. UVa/Padova simulator

The FDA approved *in silico* testing of diabetes control strategies in order to replace pre-clinical animal testing. The approved software is referred to as the *UVa/Padova simulator* and is based on the high-order model by Dalla Man et al. [19]. As this simulator is currently the most important benchmark for the evaluation of control strategies, it is important for the proposed stochastic model to perform well on data generated by this simulator.

Four different days (with scenarios defined in table 1) are generated to assess the performance on UVa simulator data. These experiments result in BG concentrations with a wide range, in such a way that the non-linearities of the UVa simulator model are not avoided. No insulin sensitivity tests are considered, because they are not compatible with the dynamics of the TPM. This is due to different steady-state behaviors between the TPM and the UVa simulator model [8].

The 10 available adults were used and basal rates were set to default values in the UVa simulator. CGM, as well as exact BG concentrations, were used for validation.

4.1.2. Clinical study

The stochastic TPM is validated on data from 10 subjects with T1DM who participated in a mono-center and open-label clinical study. A total of 7 subsequent days are available for each patient. 3 different protocols were followed: 2 insulin sensitivity test days, 2 standard therapy test days, and 3 optimized insulin infusion days. During the insulin sensitivity test days, the patients were administered isolated insulin boluses in order to be able to reliably identify the insulin sub-model of the TPM [8]. During standard therapy days, test meals were ingested and standard therapy was applied. The optimized insulin infusion days are similar to the standard therapy days with the exception that instead of an insulin bolus, an optimized insulin pattern, based on data from previous days, was administered. Additional experiment setup details are given in table 2. For some patients, some days were disregarded or shortened because of hypoglycemic interventions, medication intake, or unusually high BG variability.

The patients' basal rate was carefully tuned by physicians such that, without insulin infusions or CHO ingestion, BG stays approximately constant along the day.

d	t_s	t_e	Δ_I	t_I	Δ_M	t_M	T_M
1	8 AM	4 PM	10	8 AM	10	8 AM	10
2	8 AM	4 PM	70	8 AM	70	8 AM	20
3	8 AM	4 PM	120	8 AM	120	8 AM	10
4	8 AM	11 PM	100	10 AM	80	8 AM	10
			5	2 PM	20	2 PM	15
			10	3 PM	10	6 PM	20
			15	4 PM			

Table 1: UVa simulator protocol. Day d, experiment start time t_s, experiment end time t_e, the insulin bolus induced drop in BG Δ_I in mg/dl, the time of the insulin bolus t_I, the CHO induced rise in BG Δ_M in mg/dl, the time of the CHO intake t_M, and the meal duration T_M in minutes are given.

day	t_s	t_e	T_s	CGM	W_i
1,2	8:30 AM	11:30 AM	15	✓	5
3,4	9:00 AM	4:00 PM	30	✓	1
5,6	9:00 AM	4:00 PM	30	✓	1
7	9:00 AM	4:00 PM	30	×	1

Table 2: Clinical study protocol. The experiment start time t_s, experiment end time t_e, SMBG sampling interval T_s in minutes, availability of CGM data, and the chosen measurement point weight W_i (cf 2.3) are specified.

Measurements were taken with Accu-Chek® Combo meters for SMBG and Dexcom® SEVEN® PLUS CGMs. It should be noted that CGM data is not available on day 7.

The test meal was identical on all days and for all patients and contained 750 kcal with 25-30% carbohydrates, 15-20% protein, and 55-60% fat. This is a very slow acting meal, i.e. a meal with low GI where the rise in BG is slow, chosen intentionally to show the benefits of an insulin infusion pattern, which only exist if the insulin action is faster than the meal effect.

For model parameter identification, the weights of the different data points depend on the study day. The insulin sensitivity tests have a weight W_i that is 5 times the weight of the other days. This increased importance given to the identification quality of the insulin subsystem is key to the reliable identification of insulin action [8].

4.2. Validation methods

4.2.1. Cross-validation

The data used for parameter identification should never be used for validation. Since 4 days of UVa simulator data and 7 or 6 days for study data (for SMBG and CGM data, respectively) are available, cross-validation is performed. Model parameters are identified using the data of all but one days, while the data of the remaining day is kept for validation. This procedure is done such that every day is used for validation once. This way, a maximum of 4 validations for every adult on the UVa simulator can be obtained, which leads to a total of 40 experiments. For clinical study data, this would add up to 70 (respectively 60 for CGM data). However, since for some patients some days were disregarded, the actual number of separate validations is 58 (respectively 52 for CGM data). These results are then averaged in order to evaluate performance.

case	data origin	identification data	validation data
1	UVa simulator	exact BG	exact BG
2	UVa simulator	CGM	exact BG
3	UVa simulator	exact	CGM
4	UVa simulator	CGM	CGM
5	clinical study	SMBG	SMBG
6	clinical study	CGM	SMBG
7	clinical study	SMBG	CGM
8	clinical study	CGM	CGM

Table 3: Possible validation cases

4.2.2. Choice of identification and validation data

For each of the two data sources, two different measurements are available: the exact BG and CGM for the UVa simulator, and SMBG and CGM measurements for clinical study data. This means that there are 8 possible validation cases (cf table 3) depending on what measurements are used for identification and validation. For the sake of brevity, only a few cases are analyzed in detail.

The main goal of the proposed method is to obtain probabilistic estimations of the patient's actual BG concentration. These estimations should be as exact as possible when parameters are identified on measurements. For this reason, stochastic predictions should always be compared with the most accurate measurement that is available. Therefore, only cases 2, 5, and 6 are analyzed in detail and the other cases are used to show particular model properties.

The initialization of G and P_{BG} is always done with respect to the measurements used for identification. This means that if parameters are identified on CGM, exact, or SMBG data, then G is initialized with CGM, exact, or SMBG measurements, respectively. P_{BG} is initialized according to equation (34) with r=20%, r= 0%, or r=10%, respectively.

The way the data was collected plays a crucial role in analyzing the results. It is, for instance, straightforward to decide whether exact data generated by the UVa simulator lies within an estimated confidence interval or not. This is of course not as simple with inexact measurements, such as CGM or SMBG measurements. The measurement noise is normally distributed and the variance for SMBG and CGM measurements G_i are $\sigma_{SMBG} = \frac{0.1G_i}{1.96}$ and $\sigma_{CGM} = \frac{0.2G_i}{1.96}$, respectively. This entails that it is impossible to give an exact value for the percentage of BG concentrations within the predicted confidence interval. On the other hand, it is possible to give its expected value, denoted $p_{95\%}$. Since the exact, and not the measured BG concentration lies inside the confidence interval, is of interest, it can be assumed that $G_{e,i} \sim \mathcal{N}(G_i, \sigma_i^2)$, where $G_{e,i}$ is the exact BG concentration at time t_i. Let us denote p_i is the probability of $G_{e,i}$ being inside the confidence interval. If $\overline{x}_{BG}$ and $\underline{x}_{BG}$ are the upper and

case	% mean	% median	n
1	0	0	40
2	97.73	100	40
3	0	0	40
4	84.13	85.00	40

Table 4: Expected average and median percentage of prediction points within the 95% confidence interval on the maximum prediction horizon.

lower bounds of the estimated confidence interval, respectively, then p_i is given by the normal cumulative distribution function:

$$p_i = P(\underline{x}_{BG,i}(t) < G_{e,i} \leq \overline{x}_{BG,i}) \quad (35)$$
$$= P(G_{e,i} \leq \overline{x}_{BG,i}) - P(G_{e,i} \leq \underline{x}_{BG,i}) \quad (36)$$

, where:

$$P(X \leq a) = \frac{1}{2}\left[1 + \text{erf}\left(\frac{a - G_i}{\sqrt{2\sigma_i^2}}\right)\right] \quad (37)$$

Finally, the expected value of the percentage of points within the confidence interval is

$$p = \frac{1}{N}\sum_{i=1}^{N} p_i \quad (38)$$

If the stochastic model fulfills our assumptions and a 95% confidence interval is used, then $p \approx 95\%$.

5. Results

5.1. Percentage of measurements inside confidence interval over complete data set

First, in order to validate the proposed method for computing confidence intervals, the accuracy of the stochastic predictions over the whole duration of the available data sets (i.e. from t_s to t_e) is evaluated. Cross validation (cf 4.2.1) is performed and for every validation data set the percentage of data points within the estimated confidence interval is computed and averaged over all combinations and patients.

5.1.1. UVa simulator data

Results for cases 1 to 4, defined in table 3, are summarized in table 4 and illustrated by figure 4. Examples of simulations over the complete time horizon are given in figure 5 for different cases. Cases 1 and 2 are the most relevant ones as they compare predictions to exact BG concentrations.

- Case 1: In this case, exact measurements were used to identify model parameters. Calculating $\mathbf{Q}$ using equation (17) and $\sigma_i = 0$ for all measurements, the Fisher information matrix will be independent of both the model and the measurements. $\mathbf{Q}$ is in fact a zero matrix and, as a consequence, the stochastic term of the stochastic model is zero. Hence, the model reduces to the deterministic TPM and it is impossible to estimate confidence intervals. This can be explained by the fact that the parameter covariance matrix is assumed to be equal to the inverse Fisher information matrix even though it actually gives a lower bound on this matrix. If measurements are noiseless, this lower bound is equal to zero because, if an appropriate model is available, the model parameters can be identified perfectly. However, because of the model mismatch between the TPM and the UVa simulator model, this lower bound will not be reached. Hence, it is recommended not to use the sTPM when using exact measurements.

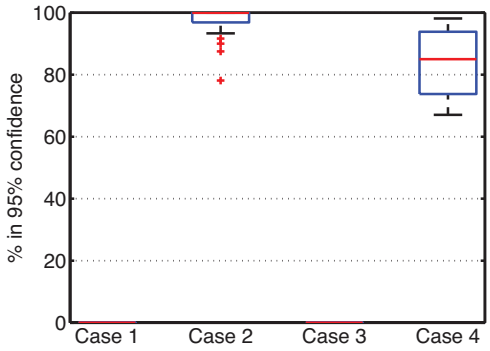

Figure 4: Boxplot of percentage of measurements inside the 95% confidence interval of all validation data sets (n=40) for cases 1-4.

- Case 2 assesses the efficiency of using CGM data for identification through comparison with exact BG concentrations. Results are very good, considering that the analysis on the maximum prediction horizon is strongly dependent on the inaccurate initial BG measurement. The percentage of points within the confidence interval is even too high, which indicates that confidence intervals may be too large. However, a visual inspection of figure 6 shows that the intervals are indeed not overly large.

  Some subjects from the UVa simulator population, such as adult 9 (which has already been identified as a complicated patient [20]), have dynamics that cannot be reproduced by the TPM. Figure 6 shows that adult 9 has a pronounced two-peak response to a meal. Hence, its dynamics are only partially captured by the TPM and the confidence intervals are only partially appropriate. The proposed method thus only performs well if the deterministic model is adapted to the data.

- Case 3 has little interest as CGM data would never be used if exact data was available. Again uncertainty is estimated to be zero, for the same reasons

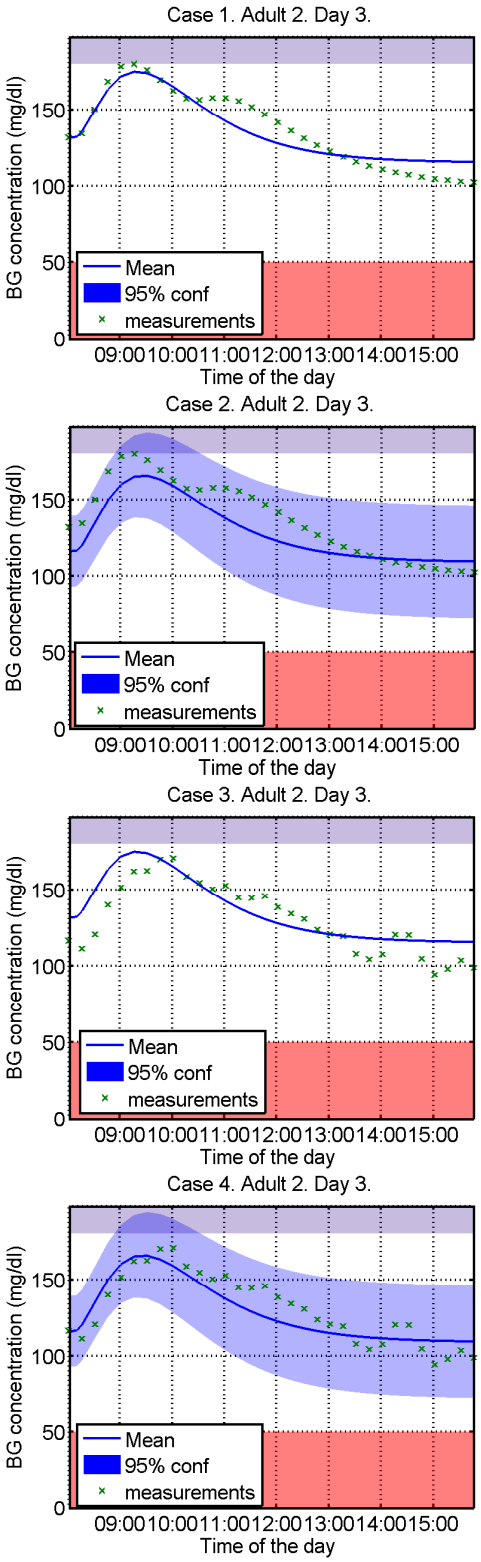

Figure 5: Examples for cases 1 (top) to 4 (bottom).

as for case 1.

- On the other hand, Case 4 is important since, in a closed-loop setting, only CGM is available. Similarly to case 2, CGM noise has a significant influence on

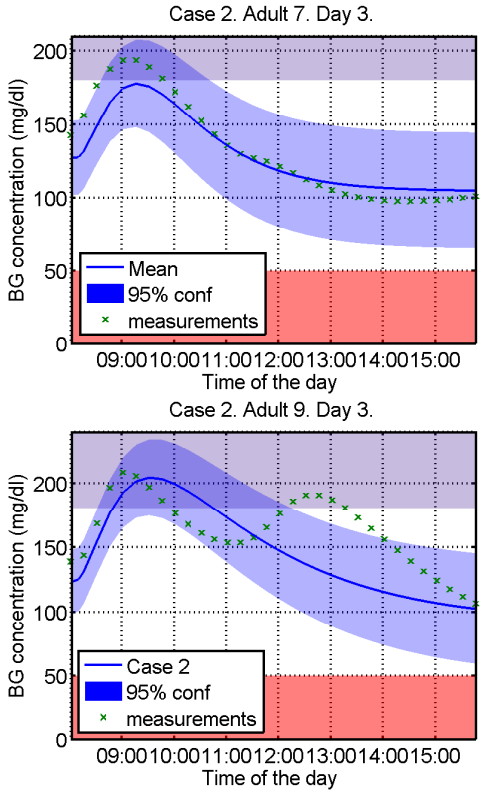

Figure 6: Examples for case 2 when validating over the complete data set.

BG initialization. Additionally, the results depend on the different noise realizations during the experiment. Since this realization is the same for all patients, the noise influence is not averaged out. Figure 7 gives an example that shows the negative influence of unfavorable noise realization, which explains the low percentage values of table 4.

Overall, the performance of the sTPM is very good on the UVa simulator when CGM data was used for identification.

5.1.2. Study data

The results of the study data analysis are summarized in table 5 and illustrated in figure 8. There is little difference between validating on SMBG and CGM data, as both measurement types have a significant level of noise. Results are generally slightly better with SMBG measurements, because of the increased confidence in the accuracy of the measurements. Only cases 5 and 6 are discussed in more detail as the observations are analogous for cases 7 and 8.

The expected percentage of points within the 95% confidence interval is acceptable for data identified using SMBG or CGM measurements. Several outliers, visible in figure 8, occur and have a strong influence on the average value. Therefore, the median, which is more robust against outliers, is also given.

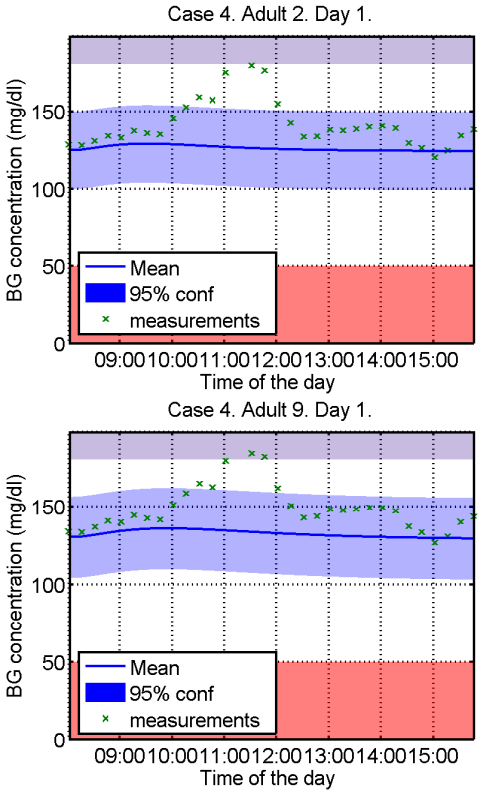

Figure 7: Examples for case 4 when validating over the complete data set. Both examples show the negative influence of their identical noise realization.

case	% mean	% median	n
5	71.25	73.38	58
6	78.80	89.68	52
7	63.58	67.38	52
8	74.80	79.67	52

Table 5: Expected average and median percentage of prediction points within the 95% confidence interval on the maximum prediction horizon.

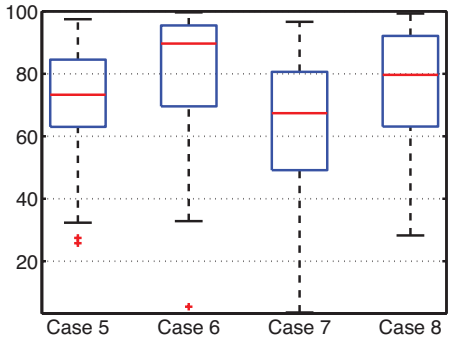

Figure 8: Boxplot of expected percentage of measurements inside the 95% confidence interval of all validation data sets for cases 5 to 8.

For case 5, results are good, but not perfect, as the expected percentage of points within the confidence interval is lower than 95%. A possible explanation is that the amplitude of the SMBG measurement noise is underestimated.

Case 6 shows better results. This is due to the fact that the assumptions on measurement noise are more appropriate. Nevertheless, results are not perfect, mainly because of the reduced quality of the parameter identification on CGM measurements. This is illustrated in figure 9: Case 5, identified on SMBG measurements, has better deterministic predictions, but narrower confidence intervals than case 6, which is identified on noisier and unreliable CGM data.

As a conclusion, with real patient data, BG uncertainty can be predicted with acceptable accuracy using SMBG, as well as CGM data. Analysis shows that, as expected, best results are obtained for parameters identified on accurate and frequently sampled data. Ideally, SMBG data with increased sampling rate or CGM data on more days should be used.

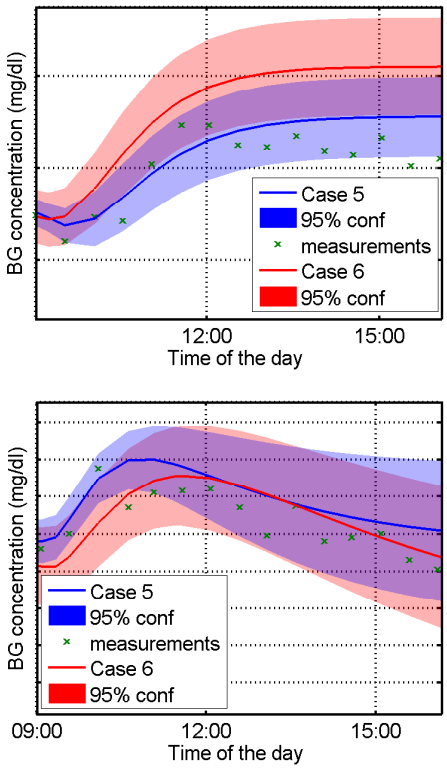

Figure 9: Comparison of stochastic prediction for cases 5 and 6.

5.2. Stochastic predictions

The analysis of the results over the maximum prediction horizon performed in section 5.1 is a good indicator for the performance of the uncertainty predictions. However, to get more insight, an analysis of the performance over well-defined prediction horizons is performed. In particular, the effects of measurement noise will be filtered out, leading to more representative results.

To do stochastic predictions, the following procedure is followed for every combination of identified model parameters and validation data set, and for every measurement G_i in the validation data set: A simulation is started h minutes before t_{G_i}, where t_{G_i} is the time of the measurement G_i and h is the prediction horizon. The inputs are propagated to initialize the insulin and CHO sub-systems and their respective covariance elements. The BG measurement preceding $t_{G_i} - h$ is used to define the initial BG and BG variance. As a consequence, to have a BG measurement to initialize the model, t_{G_i} has to be greater than $h + t_i$. The simulation is then run for h minutes and the final BG and confidence interval are compared to the measurement G_i. The results are then averaged for all measurement points, for all cross-validation permutations, and for all patients. Finally, the resulting value of points within the confidence interval and its standard deviation are plotted as a function of the prediction horizon. As illustration, examples of 90-minute predictions are given in figures 10 and 11.

The results for different prediction horizons on UVa simulator data are given in figure 12. In accordance with what was discussed in 5.1, cases 1 and 3 cannot give confidence intervals, and percentages of points within are zero. Case 2 (the most relevant one) shows excellent results over all horizons and case 4 gives good results that become even better when h increases. This improvement is due to the vanishing influence of the initial BG, and to the more favorable CGM noise realizations. The standard deviation indicates that the variability of the stochastic predictions rises with low prediction horizons and reaches a maximum value for $h > 150$ minutes. This indicates that predictions are stable, even for long horizons. The overall level of variability is acceptably small.

Figure 13 depicts the results obtained with study data. Again, these results are in agreement with section 5.1: Cases 6 and 8 have a higher percentage of points within the 95% confidence interval because the uncertainty was estimated to be larger with CGM measurements. Cases 5 and 7 show a lower percentage of points within the confidence interval, but this is caused by the SMBG measurement error that was probably larger than the used value of 10%. The quality of the predictions is very good nevertheless, as the percentage of points within the 95% confidence interval does not depend much on h. The standard deviation is shown to increase with h. This is similar to the results obtained on the UVa simulator. However, in this case, the value of the standard deviation is higher, because of the higher variability and noise level in the study data.

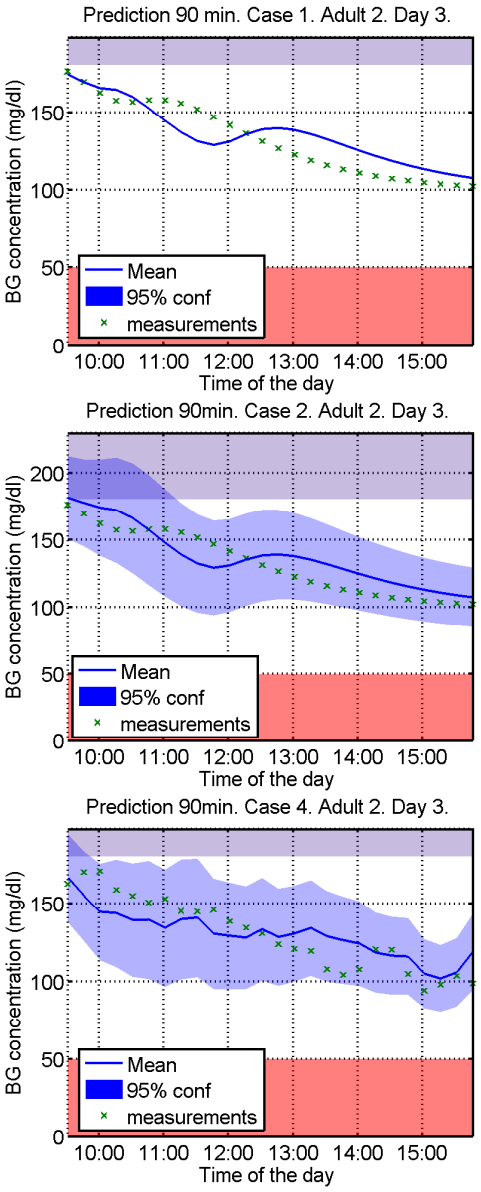

Figure 10: Examples for different cases on 90 minutes prediction horizon on UVa simulator data.

5.3. Other models

The proposed method to evaluate the prediction quality was also tested on other models (figure 14). Results on the LMM and the MM, as defined by Bock et al. [8], show acceptable results. Since LMM and MM led to inferior deterministic predictions, the performance of the corresponding stochastic model is also lower. The LMM does

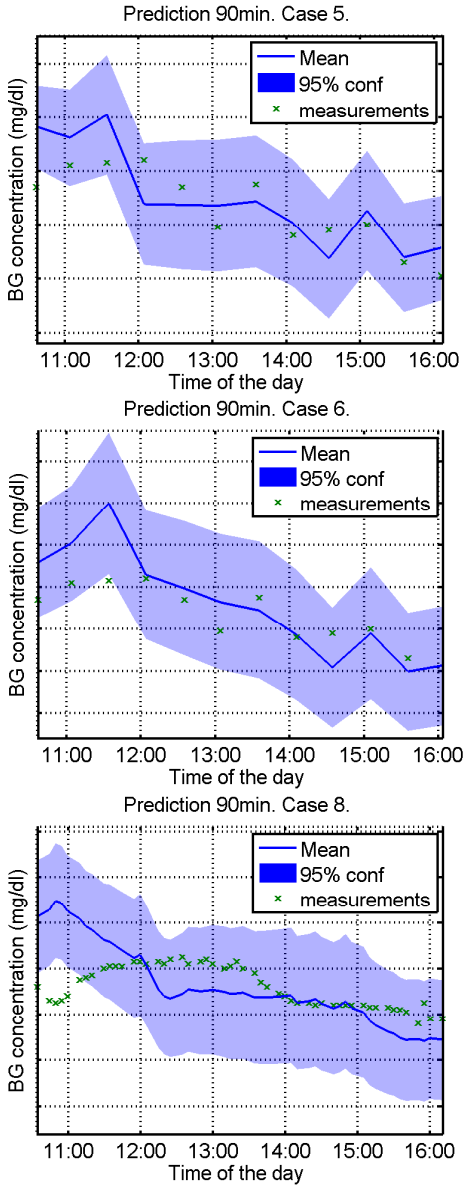

Figure 11: Examples for different cases on 90 minutes prediction horizon on clinical study data.

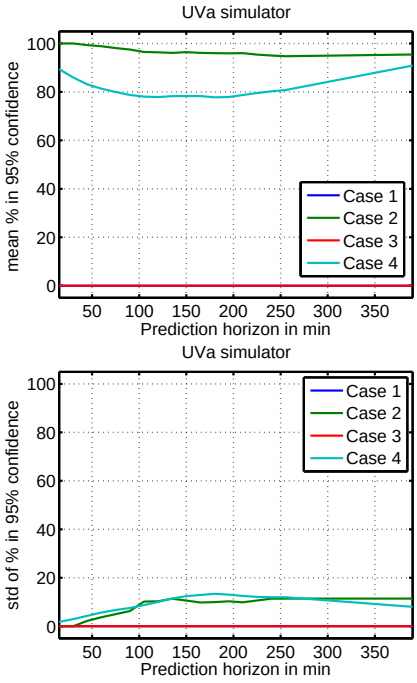

Figure 12: Prediction results for UVa simulator results (cases 1-4) for different horizons. Means and standard deviations evaluated on all 40 validation sets are given. Mean values (top) and standard deviations (bottom) are plotted.

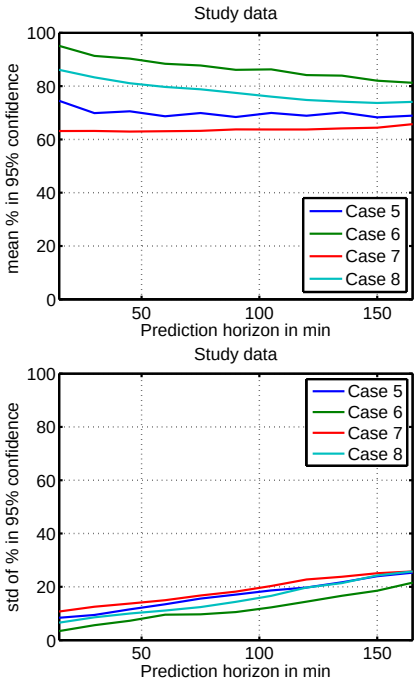

Figure 13: Prediction results for clinical study results (cases 5-8) for different horizons. Means and standard deviations evaluated on all validation sets are given. Mean values (top) and standard deviations (bottom) are plotted.

not have a linear parameterization. Therefore, the application of the EKF is an approximation. The MM is nonlinear and results in additional approximations compared to the TPM.

These results show that the method performs well even in case of mild non-linearities, especially if the deterministic model has intrinsically good prediction capabilities, but also that the quality of the deterministic model plays an important role.

6. Conclusion

A novel method, to construct a stochastic model based on parametric uncertainty and to propagate these uncertainties, was presented and applied to the TPM. This new approach allows computing confidence intervals on BG concentrations in a simple, yet effective way. It performs as expected, although the designed stochastic models are always just as good as their underlying deterministic models. As such, it is important that the latter is adapted to the modeled system. Validation was performed on UVa simulator data, as well as clinical data and led to good results for the relevant cases. Since clinical data contains more unpredictable events, estimation results were slightly worse than with UVa simulator data.

However, the expected percentage of points within the 95% confidence interval is not 95% as it should be, if all assumptions were satisfied. Hence, more than 5% of the points lie outside the estimated confidence interval. This has numerous causes, such as non-Gaussian noise, different sources of non-linearities, or exceptional intra-patient variability. Nevertheless, using the stochastic information is beneficial in all circumstances: if the uncertainty is reliably estimated, patients can be treated while considerably reducing the risks of hypo- and hyperglycemia. Furthermore, if the uncertainty is thought to be larger than it actually is, patients still have a lowered risk for large glycemic deviations, but may need to take more SMBG measurements to reduce the conservatism of the resulting recommendations for insulin injections. If uncertainties are underestimated, the treatment is still safer than without uncertainty estimations. Also, if a CGM device is used, inaccuracies can immediately be detected and parameters can be adapted accordingly.

The estimation of BG uncertainty is an invaluable addition to improve diabetes treatment. The use of the stochastic information allows reducing patient's hypo- and hyperglycemia risk, especially if combined to a CGM device. Possible new applications in the field of diabetes management are among others in predictive treatment methods (e.g. automated pancreas, pump suspension algorithms, open-loop control), state estimation, CGM filtering, detection of unexpected events, or model validation.

Future work will focus on using the proposed model for the development of tools to improve the treatment of type 1 diabetes. Furthermore, the method will be extended by the incorporation of adaptive methods to continuously

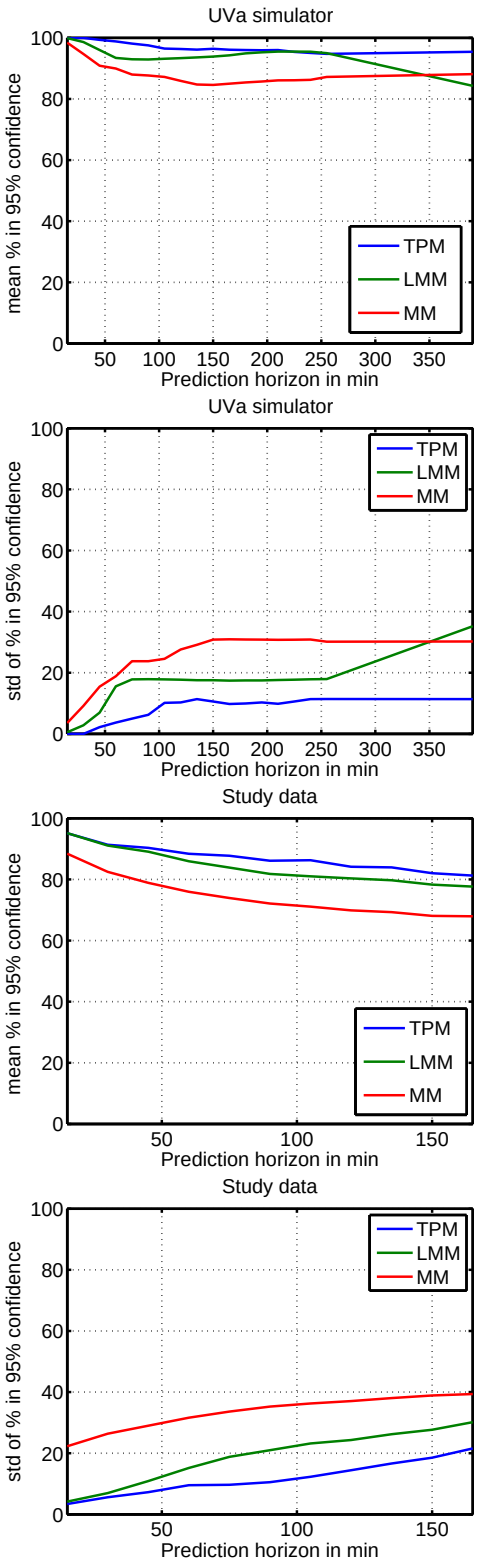

Figure 14: Stochastic prediction results for different models for case 2 and case 6. Mean values and standard deviations are plotted.

adapt model parameters to potential changes in patient's physiological characteristics. This may eventually lead to a completely automated parameter identification method.

Finally, it should be noted that the application field of this new method is not limited to diabetes management, but it may be applied to any process where a large uncertainty needs to be estimated. Also, the application is not limited to parametric uncertainty, but can be extended to take input uncertainty into account. Coming back to BG control, the uncertainty in the estimation of meal amounts could also be addressed.

Acknowledgment

The authors acknowledge the financial support from Roche Diagnostic Diabetes Care. We would also like to thank Dr. Abhishek Soni for helpful comments and suggestions. Thanks to Florent Xavier for testing the proposed method during a semester project.

Appendix A. Stochastic TPM equations

The covariance propagation equations for the TPM are given below. If combined with the deterministic TPM equations 20 to 24, the complete stochastic model can be simulated.

$$\begin{aligned}\dot{P}_{G,G} =&Q_{K_x,K_x}X^2 - 2Q_{K_g,K_x}XU_G \\ &+ Q_{K_g,K_g}U_G^2 + 2K_gP_{G,U_G} - 2K_xP_{G,X}\end{aligned} \tag{A.1}$$

$$\begin{aligned}\dot{P}_{G,U_G} =&K_gP_{U_G,U_G} - K_xP_{U_G,X} - a_gP_{G,U_G} \\ &+ a_gP_{U_G,U_{G,1}} + XQ_{a_g,K_x}(U_G - U_{G,1}) \\ &- U_GQ_{K_g,a_g}(U_G - U_{G,1})\end{aligned} \tag{A.2}$$

$$\begin{aligned}\dot{P}_{U_G,U_G} =&2a_gP_{U_G,U_{G,1}} - 2a_gP_{U_G,U_G} \\ &+ Q_{a_g,a_g}(U_G - U_{G,1})^2\end{aligned} \tag{A.3}$$

$$\begin{aligned}\dot{P}_{G,U_{G,1}} =&K_gP_{U_G,U_{G,1}} - K_xP_{U_{G,1},X} - a_gP_{G,U_{G,1}} \\ &- XQ_{a_g,K_x}(U_{CHO} - U_{G,1}) \\ &+ U_GQ_{K_g,a_g}(U_{CHO} - U_{G,1})\end{aligned} \tag{A.4}$$

$$\begin{aligned}\dot{P}_{U_G,U_{G,1}} =&a_gP_{U_{G,1},U_{G,1}} - 2a_gP_{U_G,U_{G,1}} \\ &- Q_{a_g,a_g}(U_{CHO} - U_{G,1})(U_G - U_{G,1})\end{aligned} \tag{A.5}$$

$$\dot{P}_{U_{G,1},U_{G,1}} =Q_{a_g,a_g}(U_{CHO} - U_{G,1})^2 - 2a_gP_{U_{G,1},U_{G,1}} \tag{A.6}$$

$$\begin{aligned}\dot{P}_{G,X} =&K_gP_{U_G,X} - K_xP_{X,X} - a_xP_{G,X} + a_xP_{G,X_1} \\ &+ XQ_{K_x,a_x}(X - X_1) - U_GQ_{K_g,a_x}(X - X_1)\end{aligned} \tag{A.7}$$

$$\begin{aligned}\dot{P}_{U_G,X} =&a_gP_{U_{G,1},X} - a_gP_{U_G,X} - a_xP_{U_G,X} + a_xP_{U_G,X_1} \\ &+ P_{U_G,X}(X - X_1)(U_G - U_{G,1})\end{aligned} \tag{A.8}$$

$$\begin{aligned}\dot{P}_{U_{G,1},X} =&a_xP_{U_{G,1},X_1} - a_xP_{U_{G,1},X} - a_gP_{U_{G,1},X} \\ &- P_{U_G,X}(X - X_1)(U_{CHO} - U_{G,1})\end{aligned} \tag{A.9}$$

$$\dot{P}_{X,X} =2a_xP_{X,X_1} - 2a_xP_{X,X} + Q_{a_x,a_x}(X - X_1)^2 \tag{A.10}$$

$$\begin{aligned}\dot{P}_{G,X_1} =&K_gP_{U_G,X_1} - K_xP_{X,X_1} - a_xP_{G,X_1} \\ &+ XQ_{K_x,a_x}(X_1 - U_I) - U_GQ_{K_g,a_x}(X_1 - U_I)\end{aligned} \tag{A.11}$$

$$\begin{aligned}\dot{P}_{U_G,X_1} =&a_gP_{U_{G,1},X_1} - a_gP_{U_G,X_1} - a_xP_{U_G,X_1} \\ &+ Q_{a_g,a_x}(X_1 - U_I)(U_G - U_{G,1})\end{aligned} \tag{A.12}$$

$$\begin{aligned}\dot{P}_{U_{G,1},X_1} =&- a_gP_{U_{G,1},X_1} - a_xP_{U_{G,1},X_1} \\ &- Q_{a_g,a_x}(X_1 - U_I)(U_{CHO} - U_{G,1})\end{aligned} \tag{A.13}$$

$$\begin{aligned}\dot{P}_{X,X_1} =&a_xP_{X_1,X_1} - 2a_xP_{X,X_1} \\ &+ Q_{a_x,a_x}(X - X_1)(X_1 - U_I)\end{aligned} \tag{A.14}$$

$$\dot{P}_{X_1,X_1} =Q_{a_x,a_x}(X_1 - U_I)^2 - 2a_xP_{X_1,X_1} \tag{A.15}$$

References

[1] The Diabetes Control and Complications Trial Research Group, The effect of intensive treatment of diabetes on the development and progression of long-term complications in insulin-dependent diabetes mellitus., New Engl J Med 329 (14) (1993) 977–86. doi:10.1056/NEJM199309303291401.

[2] L. Heinemann, Variability of insulin absorption and insulin action, Diabetes Technol. Ther. 4 (5) (2002) 673–682.

[3] J. Vora, T. Heise, Variability of glucose-lowering effect as a limiting factor in optimizing basal insulin therapy. A review., Diabetes. Obes. Metab.doi:10.1111/dom.12087.

[4] G. Freckmann, A. Baumstark, N. Jendrike, E. Zschornack, S. Kocher, J. Tshiananga, F. Heister, C. Haug, System accuracy evaluation of 27 blood glucose monitoring systems according to DIN EN ISO 15197, Diabetes Technol. Ther. 12 (3) (2010) 221–31.

[5] G. Freckmann, S. Pleus, M. Link, E. Zschornack, H.-M. Klötzer, C. Haug, Performance evaluation of three continuous glucose monitoring systems: comparison of six sensors per subject in parallel, J. Diabetes Sci. Technol. 7 (4) (2013) 842–853.

[6] J. Kildegaard, J. Randlø v, J. U. Poulsen, O. K. Hejlesen, The impact of non-model-related variability on blood glucose prediction, Diabetes Technol. Ther. 9 (4) (2007) 363–71. doi:10.1089/dia.2006.0039.

[7] T. Prud'homme, A. Bock, G. Francois, D. Gillet, Preclinically assessed optimal control of postprandial glucose excursions for type 1 patients with diabetes, in: 2011 IEEE Int. Conf. Autom. Sci. Eng., IEEE, 2011, pp. 702–707. doi:10.1109/CASE.2011.6042510.

[8] A. Bock, G. François, D. Gillet, A Therapy Parameter-based Model for Predicting Blood Glucose Concentrations in Patients with Type 1 Diabetes, Comput. Methods Programs Biomed.

[9] E. Dassau, P. Herrero, H. Zisser, B. A. Buckingham, L. Jovanovič, C. D. Man, C. Cobelli, J. Vehí, F. J. Doyle III, Implications of Meal Library & Meal Detection to Glycemic Control of Type 1 Diabetes Mellitus through MPC Control, in: 17th IFAC World Congr., Seoul, Korea, 2008, pp. 4228–4233.

[10] M. García-Jaramillo, R. Calm, J. Bondia, J. Vehí, Prediction of postprandial blood glucose under uncertainty and intra-patient variability in type 1 diabetes: A comparative study of three interval models, Comput. Methods Programs Biomed.doi:10.1016/j.cmpb.2012.04.003.

[11] E. Gardeñes, M. A. Sainz, L. Jorba, R. Calm, R. Estela, H. Mielgo, A. Trepat, Modal Intervals, Reliab. Comput. 7 (2001) 77–111.

[12] H. Kirchsteiger, S. Pölzer, R. Johansson, E. Renard, L. del Re, Direct continuous time system identification of MISO transfer function models applied to type 1 diabetes, IEEE Conf. Decis. Control Eur. Control Conf. (1) (2011) 5176–5181. doi:10.1109/CDC.2011.6161344.

[13] S. Klim, Predictive tools for designing new insulins and treatment regimens, Ph.D. thesis, DTU (2009).

[14] F. Cameron, Explicitly Minimizing Clinical Risk through Closed-loop Control of Blood Glucose in Patients with Type 1 Diabetes Mellitus, Ph.D. thesis, Stanford University (2010).

[15] F. Cameron, G. Niemeyer, K. Gundy-Burlet, B. Buckingham, Statistical hypoglycemia prediction., J. Diabetes Sci. Technol. 2 (4) (2008) 612–21.

[16] C. L. Zhang, F. A. Popp, Log-normal distribution of physiological parameters and the coherence of biological systems, Med. Hypotheses 43 (1) (1994) 11–16. doi:10.1016/0306-9877(94)90042-6.

[17] D. Simon, Optimal State Estimation: Kalman, H Infinity, and Nonlinear Approaches, Vol. 54, Wiley-Interscience, 2006.

[18] E. R. Damiano, F. H. El-Khatib, Z. H, D. M. Nathan, S. J. Russell, A Comparative Effectiveness Analysis of Three Continuous Glucose Monitors, Diabetes Caredoi:10.2337/dc12-0070.

[19] C. Dalla Man, D. M. Raimondo, R. A. Rizza, C. Cobelli, GIM, simulation software of meal glucose-insulin model., J. Diabetes Sci. Technol. 1 (3) (2007) 323–30.

[20] F. Cameron, B. W. Bequette, D. M. Wilson, B. A. Buckingham, H. Lee, G. Niemeyer, A Closed-Loop Artificial Pancreas Based on Risk Management, J. Diabetes Sci. Technol. 5 (2) (2011) 368–379.